SEMARAK ILMU PUBLISHING

Journal of Advanced Research in Numerical Heat Transfer

Journal homepage:
https://semarakilmu.com.my/journals/index.php/arnht/index
ISSN: 2735-0142

CFD Analysis of Indoor Ventilation for Airborne Virus Infection

Kaishan Feng[1], Yoshiki Yanagita[1], Yuko Miyamura[1,2], Adi Azriff Basri[3], Mohammad Zuber[4], Siti Rohani[5], Kamarul Arifin Ahmad[3], Masaaki Tamagawa[1,*]

[1] Graduate School of Life Science System and Engineering, Kyushu Institute of Technology, Hibikino 2-4, Wakamatsu-ku, Kitakyushu, Fukuoka 808-0196, Japan
[2] Department of Nursing, Faculty of Fukuoka Medical Technology, Teikyo University Misaki-machi 6-22, Omuta, Fukuoka 836-8505, Japan
[3] Department of Aerospace Engineering, Faculty of Engineering, Universiti of Putra Malaysia, 43400 Serdang, Selangor, Malaysia
[4] Department of Aeronautical and Automobile Engineering, Manipal Institute of Technology, Manipal Academy of Higher Education (MAHE), 75150 Melaka, Malaysia
[5] Hospital Kuala Lumpur, Jalan Pahang, 50586 Kuala Lumpur, Malaysia

ARTICLE INFO

Article history:
Received 1 June 2023
Received in revised form 5 July 2023
Accepted 7 August 2023
Available online 1 September 2023

Keywords:
Infection prevention; Ventilation; CFD; Residence time; Aerosols

ABSTRACT

Indoor airflow patterns and air residence times significantly influence the spread of airborne infectious viruses, such as COVID-19. These factors can be quantified using computational fluid dynamics (CFD). In this study, CFD was utilized to assess the indoor airflow patterns and calculate air residence times in a typical restroom with high personnel flow and low ventilation efficiency. The results identified regions with high air residence times, indicating potential risk areas for airborne virus retention. Furthermore, the effects of different ventilation strategies on these high-risk areas were analyzed. Despite meeting air change standards, certain regions were found to potentially pose a higher risk due to prolonged air residence times. Based on these findings, recommendations for improving ventilation systems to reduce the risk of airborne virus infection were proposed. This study highlights the necessity of a more nuanced approach to indoor air assessment than simply calculating air changes per hour. It was concluded that (1) different ventilation strategies can greatly affect the air residence time in the room and (2) the variance of air residence time in the air circulation area are large in some locations, even with simple ventilation adjustments.

1. Introduction

The transmission of airborne infectious viruses such as COVID-19 is predominantly propelled by the emission of aerosols during activities like sneezing, coughing, or talking. Sinha *et al.,* [1] pointed out that recirculating air flow present at corners and around obstacles can trap air and infectious aerosol. This constitutes a significant threat to public health, particularly within indoor environments where virus-laden aerosols can linger in the air for extensive periods.

Several authors assessed the infection risk in indoor spaces by evaluating the frequency of air changes per hour is often used as an indicator [2-4]. However, this approach can present notable

[*] *Corresponding author.*
E-mail address: tama@life.kyutech.ac.jp (Masaaki Tamagawa)

https://doi.org/10.37934/arnht.14.1.116

limitations, as it fails to account for the presence of recirculation zones within a room, such as corners or areas near obstructions that have been demonstrated by other authors [5-9]. Besides, some authors have proved that these zones can harbor aerosols for prolonged periods, thereby exposing individuals within these areas to an elevated risk of infection, even in instances where overall ventilation efficiency is deemed sufficient [10-16]. Addressing these limitations necessitates the investigation of airflow patterns within indoor environments and the identification of areas with high air residence time.

Computational fluid dynamics (CFD) simulations facilitate an analysis of air velocity vectors and air residence time to understand airflow patterns within restrooms. By juxtaposing recirculation zones with the locations of high air residence time, the correlation between air velocity and air residence time can be established. This information can subsequently be leveraged to pinpoint areas within the restroom where occupants are most susceptible to COVID-19 infection.

The present study utilizes Computational Fluid Dynamics (CFD) to investigate airflow patterns in two disparate high-traffic restrooms, which are inherently plagued by poor ventilation efficiencies and the existence of physical obstructions. Existing literature, such as the work of Li *et al.,* [17] has underscored the potential role that toilets can play in promoting virus transmission. This underlines a substantial gap in the current understanding of the relationship between restroom design, ventilation systems, and the spread of airborne pathogens, emphasizing the pressing need for further examination. The significance of this study resides in its potential to provide novel insights into the influence of architecture and ventilation strategies on air residence time and infection risk.

2. Methodology

2.1 Governing Equations

To analyse fluid motions in the models, the continuum equation and incompressible Navier-Stokes equation are used as the governing equations:

$$\frac{\partial \rho}{\partial t} + \nabla \cdot (\rho U) = 0 \tag{1}$$

$$\frac{\partial}{\partial t}(\rho U) + \nabla \cdot (\rho U U) = -\nabla p + \mu \Delta \cdot U + \rho g \tag{2}$$

where t is time, $\boldsymbol{U}$ is velocity vector, p is static pressure, μ is viscosity of air, ρ is density of air, g is gravity worked for only y-axis direction. In this study, the air is incompressible fluid. As for the turbulent model, the Realizable "k-ε " model is used.

The research presented herein underscores that the airflow from the windows yielded a temperature lower than that of the room. Consequently, the air flow within the chamber is classified as non-isothermal. For such instances, it becomes essential to account for temperature transmission, as illustrated by the ensuing formula:

$$\frac{\partial}{\partial t}(\rho T) + \boldsymbol{\nabla} \cdot (\rho \boldsymbol{U}\, T) - \boldsymbol{\nabla} \cdot \{(\lambda_L + \lambda_t)\, \boldsymbol{\nabla} T\} = S_T \tag{3}$$

where T is temperature, S_T is the source term of temperature, λ_L=2.05×10^{-5}m^2/s is the laminar diffusion coefficient, turbulence diffusion coefficient $\lambda_t$is calculated by:

$$\lambda_t = \frac{\upsilon_t}{Sc_t} \tag{4}$$

where the turbulent Schmidt number Sc_t is difficult to obtain by the experiment for the current study. Using 0.7 in indoor ventilation is agreed by Toja-Silva *et al.,* [18] in related similar experimental results.

To obtain the volume-averaged residence time in the male restroom model, local volume-averaged residence time defined by the following equation can be used:

$$\frac{\partial}{\partial t}(\rho\tau_i) + \nabla\cdot(\rho \boldsymbol{U}\tau_i) = S_\tau \tag{5}$$

where i is the number of each computational cell, τ_i is residence time for i-th computational cell, S_τ is the source term of residence time. To evaluate the ventilation efficiency, the volume-averaged residence time in the room is used by following equation:

$$\bar{\tau} = \frac{1}{V}\int \tau \, dV = \frac{\sum(\tau_i \times \Delta v_i)}{V} \tag{6}$$

where $\bar{\tau}$ is volume-averaged residence time, V is volume of the model, Δv_i is the volume in i-th computational cell. By using Eq. (6), $\bar{\tau}$ will be evaluated with changing Δv_i and τ in the following section.

2.2 Boundary Conditions

The influence of ventilation on air residence time and the correlated risk of viral transmission is assessed using two simplified computational models grounded on fundamental air flow equations. These models are constructed to mirror real-world restroom environments, factoring in their size, structural attributes, and ventilation setups. Comparing the outcomes of Model 1 and Model 2 allows the discernment of the impact of partition walls and windows on air residence time.

The models, are illustrated in Figure 1 and Figure 2, including Model 1 and Model 2, which each consider different window status scenarios (either closed or opened).

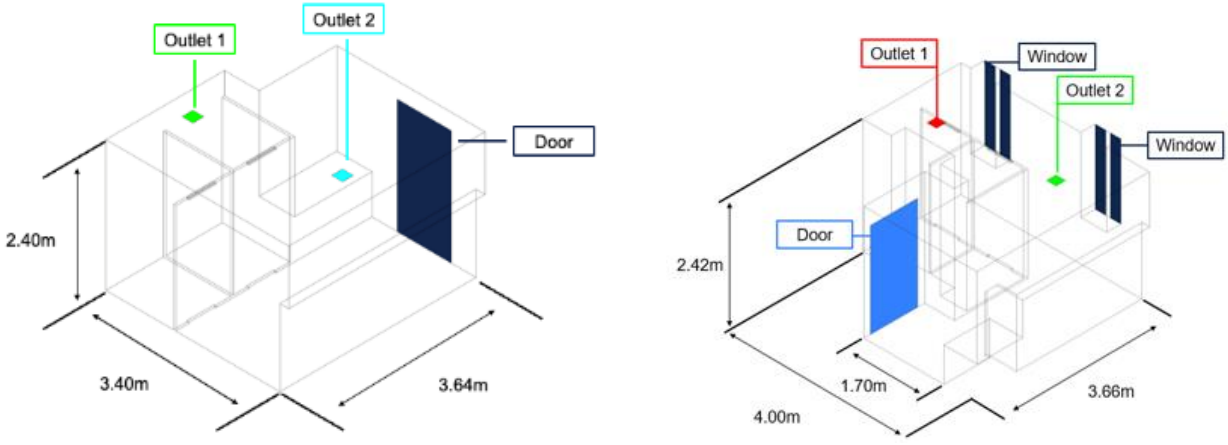

(a) (b)

Fig. 1. The structure of (a) Model 1 (b) Model 2

Model 1 and Model 2, with the windows closed, are utilized to analyze the distribution of air residence time in restrooms featuring a variety of structural configurations. The effect of enhanced ventilation strategies is examined in Model 2 with windows opened. The flow rate and temperature for each scenario are detailed in Table 1, Table 2, and Table 3. In both Model 1 and the closed-window

variant of Model 2, airflow is presumed to enter through the door and exit through outlets, with the wall regarded as adiabatic, negating any heat transfer. No heat sources are present at the outlets, and additional boundary conditions are established based on gathered data or device specifications.

Table 1
Boundary conditions for Model 1

Place	Flow rate	Temperature
Outlet1	4.6 [m^3/min]	23.0 [℃]
Outlet2	4.6 [m^3/min]	23.0 [℃]
Door (Inlet)	9.2 [m^3/min]	23.0 [℃]
Wall	0.0 [m^3/min]	$\partial T/\partial n$ = 0 [℃/m]

Table 2
Boundary conditions for Model 2 (windows closed)

Place	Flow rate	Temperature
Outlet1	4.6 [m^3/min]	27.0 [℃]
Outlet2	4.6 [m^3/min]	27.0 [℃]
Window1 (Inlet)	0.0 [m^3/min]	$\partial T/\partial n$ = 0 [℃/m]
Window2 (Inlet)	0.0 [m^3/min]	$\partial T/\partial n$ = 0 [℃/m]
Door (Inlet)	9.2 [m^3/min]	27.0 [℃]
Wall	0.0 [m^3/min]	$\partial T/\partial n$ = 0 [℃/m]

Table 3
Boundary conditions for Model 2 (windows opened)

Place	Flow rate	Temperature
Outlet1	4.6 [m^3/min]	27.0 [℃]
Outlet2	4.6 [m^3/min]	27.0 [℃]
Window1 (Inlet)	25.0 [m^3/min]	17.0 [℃]
Window2 (Inlet)	25.0 [m^3/min]	17.0 [℃]
Door (Inlet)	59.2 [m^3/min]	27.0 [℃]
Wall	0.0 [m^3/min]	$\partial T/\partial n$ = 0 [℃/m]

3. Results

3.1 Reference Planes and Monitoring Points

Figure 2 illustrates the establishment of two reference planes that aid in visualizing the spread of health-threatening aerosols. A horizontal plane, placed at a height of 1.7 meters from the ground, symbolizing the nose height of an average male, is chosen as the primary reference plane in Figure 2(a). In addition, to evaluate indoor air quality, a secondary reference plane is required to analyze the relationship between air recirculation and air residence time as shown in Figure 2(b). These reference planes will help in better understanding the dynamics of airborne aerosol movement within indoor environments.

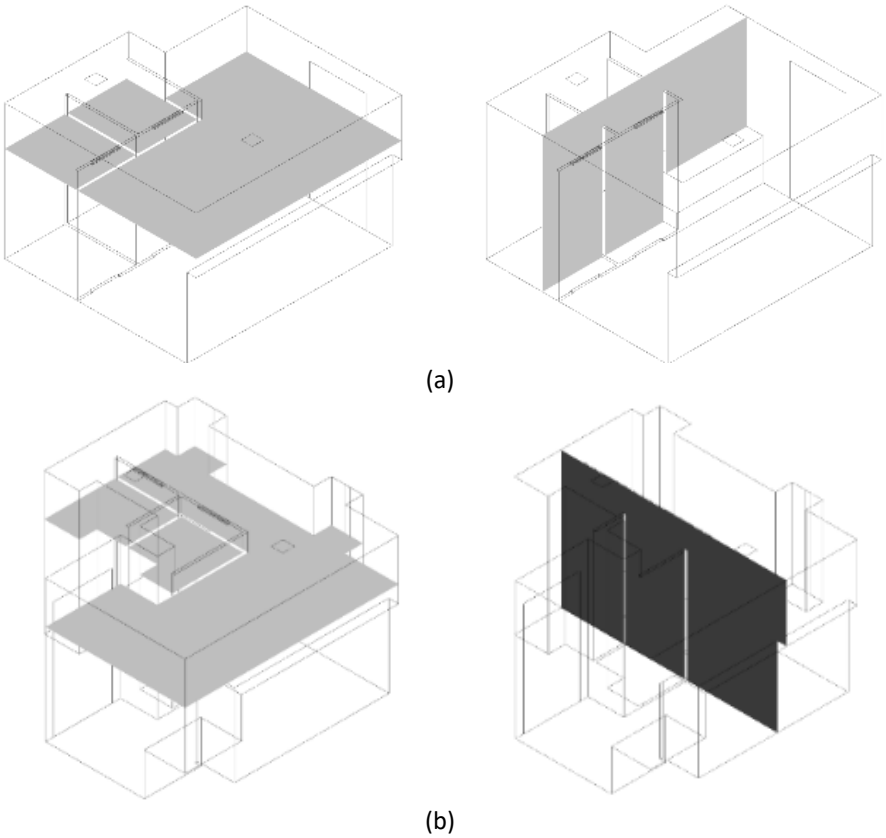

Fig. 2. The reference planes for model 1 and model 2 (a) The horizontal and the vertical reference plane of Model 1 (b) The horizontal and the vertical reference plane of Model 2

Figure 3 illustrates the computational mesh developed for Models 1 and 2. The models consist of 386,254 and 431,926 cells, respectively, subdivided using the Poly-Hexcore meshing method. This method integrates the benefits of hexahedral and polygonal grids, allowing for efficient handling of complex geometries and polygonal boundaries while retaining the consistency and effectiveness of hexahedral grids. The Poly-Hexcore technique primarily involves the formation of boundary polygons based on a hexahedral grid to encapsulate the surface of hexahedral cells.

When assessing mesh partition quality, skewness, a measure of the distortion of the cell shape, is considered under the physics preferences. This is crucial to ensure the accuracy and stability of the simulation. Due to the simulation software's cell number limit (524,000), a grid independence test wasn't conducted. Nonetheless, the number of cells used in these models should provide a reasonable balance between accuracy and computational efficiency

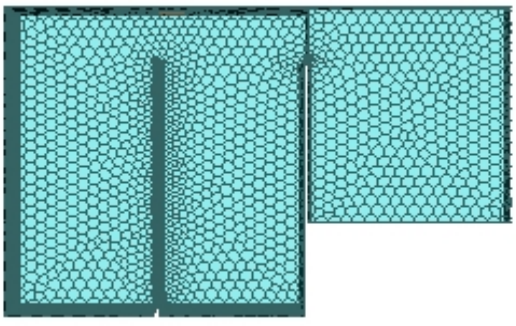

Fig. 3. The mesh method in the models

Placement of the monitoring points was undertaken with the aim of accurately assessing air distribution and its resultant effect on human exposure. The derived data from these points underwent analysis with regard to air residence time, a term defining the duration for which air remains in a particular environment. For a comprehensive assessment of potential infection risks from airborne aerosols within the partitions, monitoring points were set up in every partition across both models. Their positions, as illustrated in Figures 4(a) and Figure 4(b), correspond to the location of an adult male's nose when in a squatting position.

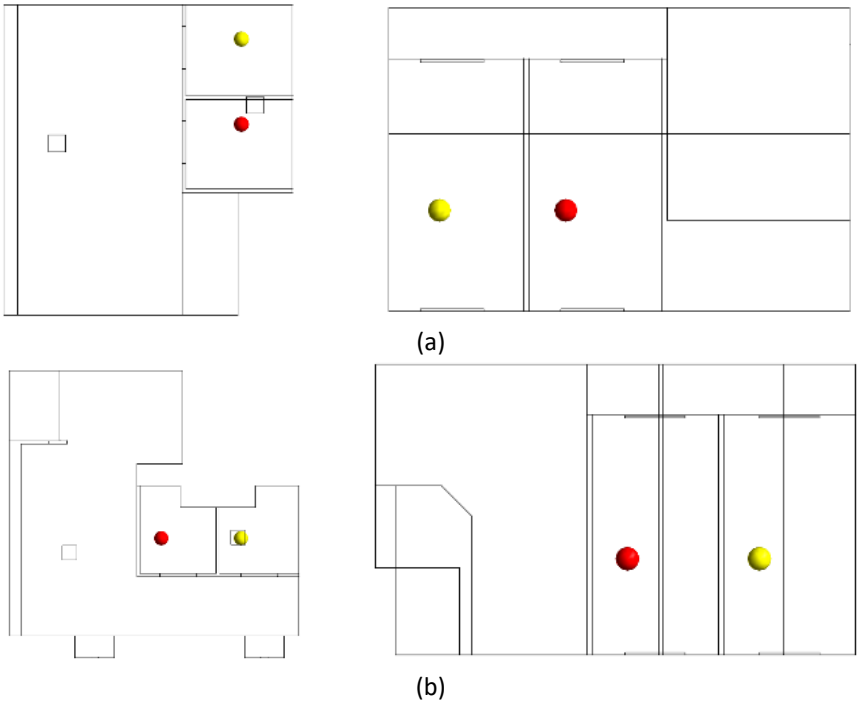

Fig. 4. The positions of two monitoring point for model 1 (a) The positions of monitoring point 1 (yellow) from the top view and monitoring point 2 (red) from the main view of Model 1 (b) The positions of monitoring point 1 (yellow) from the top view and monitoring point 2 (red) from the main view of Model 2

3.2 Distribution of the Airflow Streamlines

The simulation aimed to observe the system's behaviour over an extended duration. Spanning 540 seconds, this simulation facilitated the exploration of significant changes over time. For comparative purposes, the volume-averaged residence time was calculated, correlating the simulated results with real-world data. The comparative findings are graphically represented in Figure 5.

Notably, the simulation attained a steady state beyond the 300-second mark. The term 'steady state' indicates a point of stability within the system where parameter changes become negligible. Once this steady state was achieved, the volume-averaged residence time remained largely constant, experiencing a consistent decrease as the calculation time extended. It is anticipated that this diminishing trend will persist with the continuation of the simulation, rendering the results at the 540-second mark of utmost importance for subsequent analysis and discourse. This 540-second mark thus potentially offers the most stable fluid field in the study.

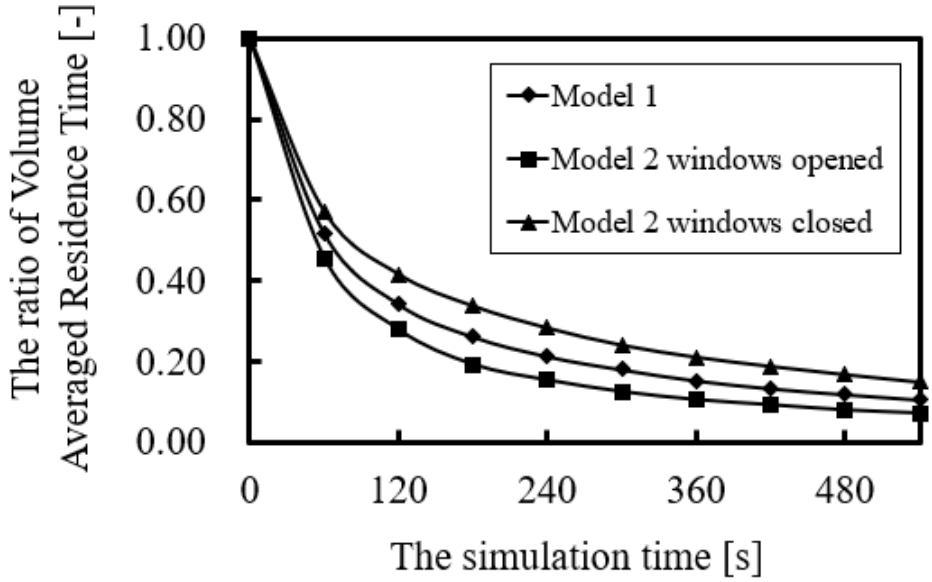

Fig. 5. The ratio of Volume Averaged Residence Time and calculation time in different models

For a comprehensive understanding of the entire airflow pathway, it is necessary to analyze the distribution of streamlines. As illustrated in Figure 6, fresh air enters the room from outside the model. The outcomes of Model 1 and Model 2, with windows closed, reveal that reliance on fresh air inflow solely through the door has a limited effect on indoor air quality enhancement, especially in complex interior structures with few areas open to improvement. The disparity between cases with closed and opened windows in Model 2 emphasizes the importance of ventilation inlets that allow fresh air into the room. With the windows opened, areas previously inaccessible to the fresh air flow now receive ventilation from the windows. Even partitions enclosed by walls receive partial fresh air supply.

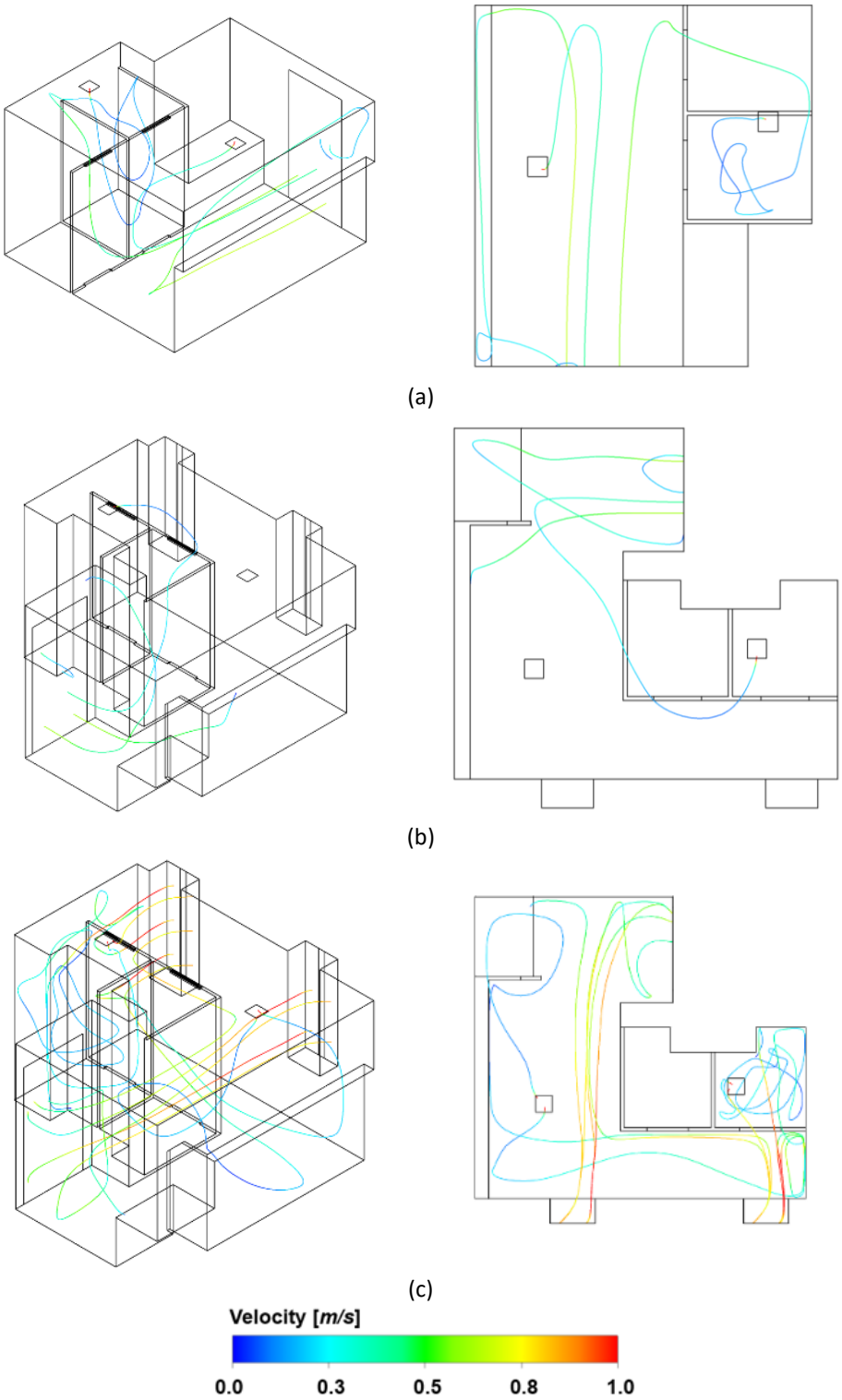

Fig. 6. Streamlines in (a) Model 1 (b) Model 2 (windows are closed) (c) Model 2 (windows are opened)

3.3 Distribution of the Velocity Vector

Figure 7 to Figure 9 presents the velocity vectors of airflow within the different models. Analyzing the distribution of these vectors aids in understanding the relationship between airflow recirculation

and air residence time. To investigate the airflow in the two partitions of each case, the velocity vector distributions at the top and bottom of each partition are selected.

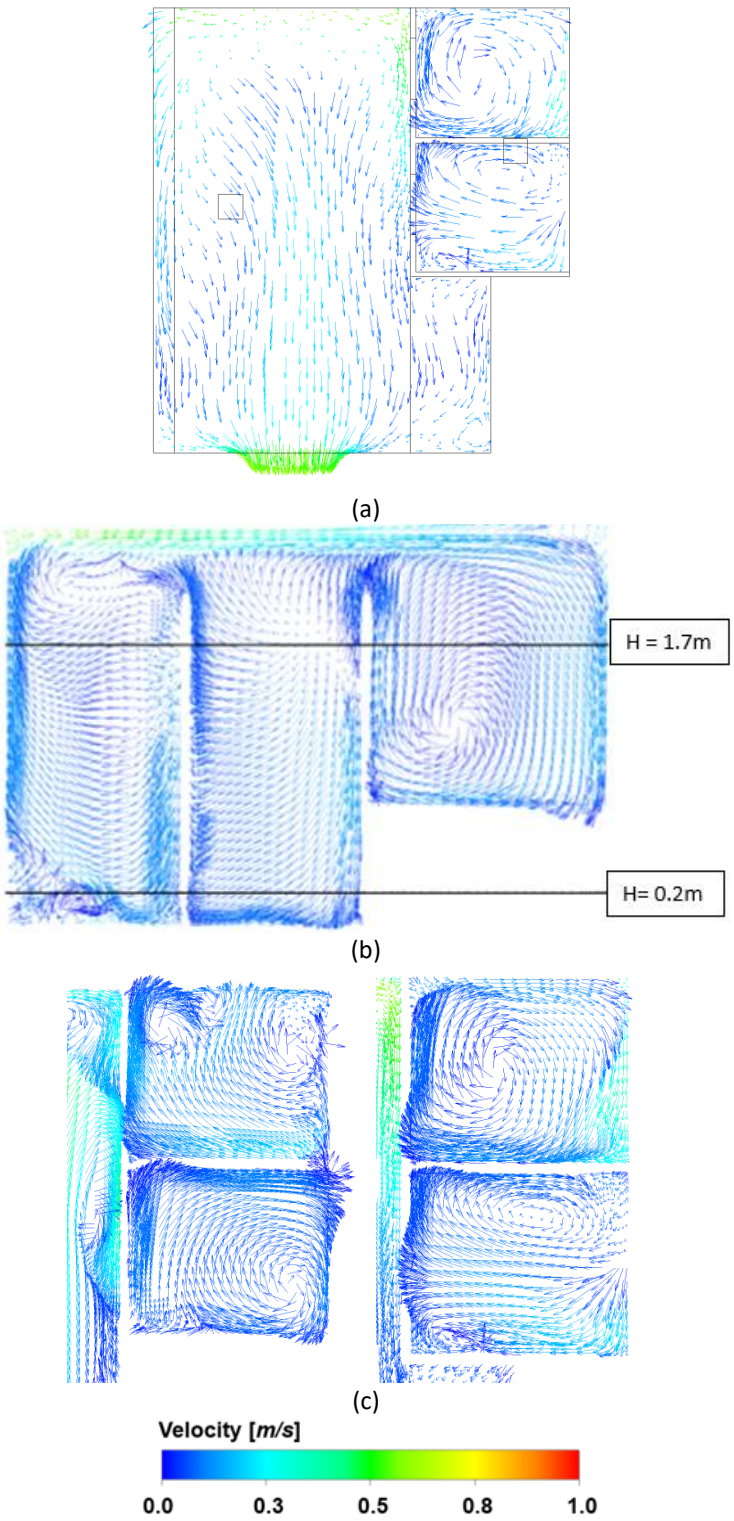

Fig. 7. The distribution of airflow velocity vector in Model 1 (a) Airflow velocity vectors on the horizontal plane (b) Airflow velocity vectors on the vertical plane (c) Airflow velocity vectors on the horizontal plane at H=1.7m and H=0.2m

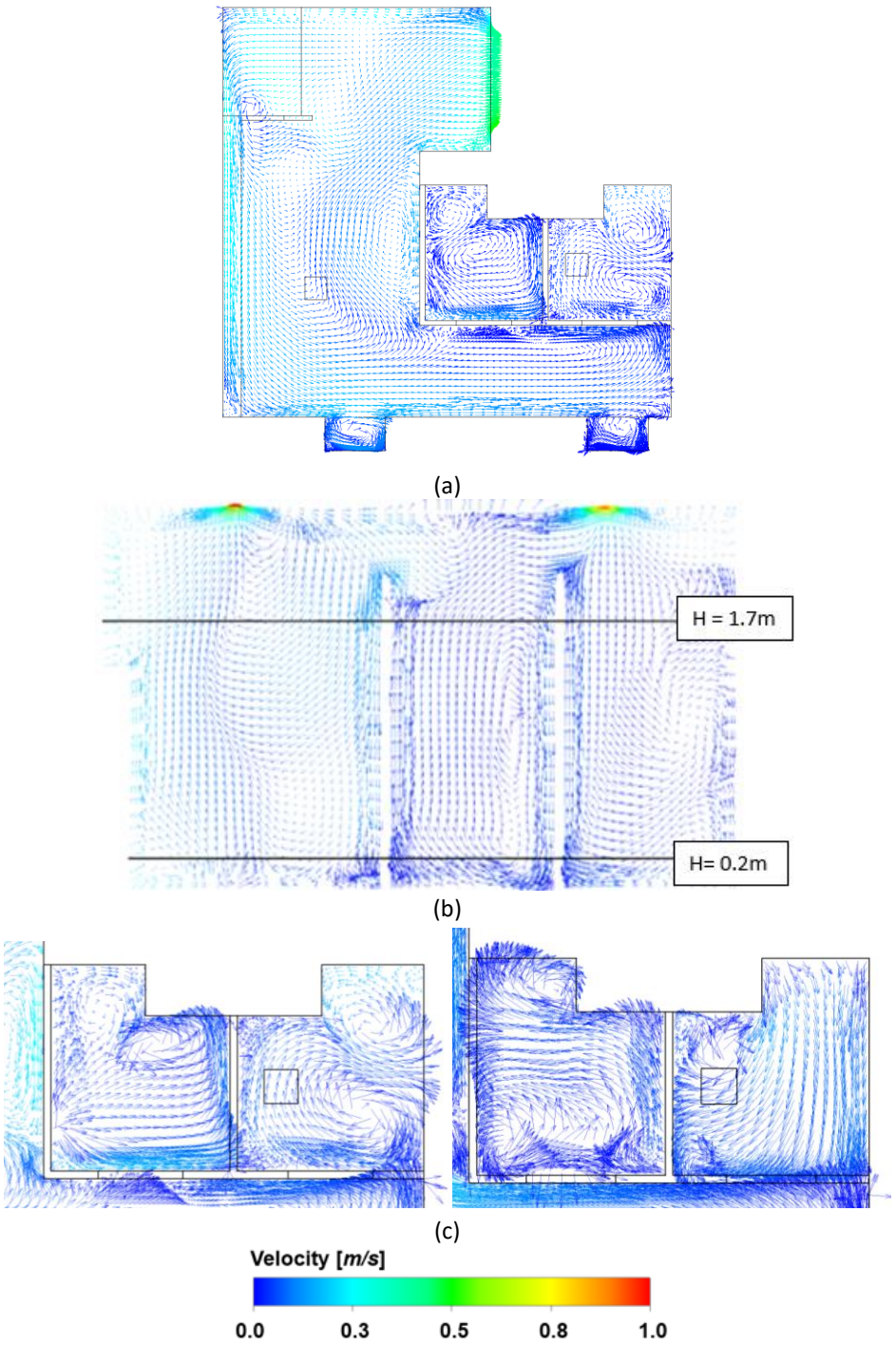

Fig. 8. The distribution of airflow velocity vector in Model 2 (windows are closed) (a) Airflow velocity vectors on the horizontal plane (b) Airflow velocity vectors on the vertical plane (c) Airflow velocity vectors on the horizontal plane at H=1.7m and H=0.2m

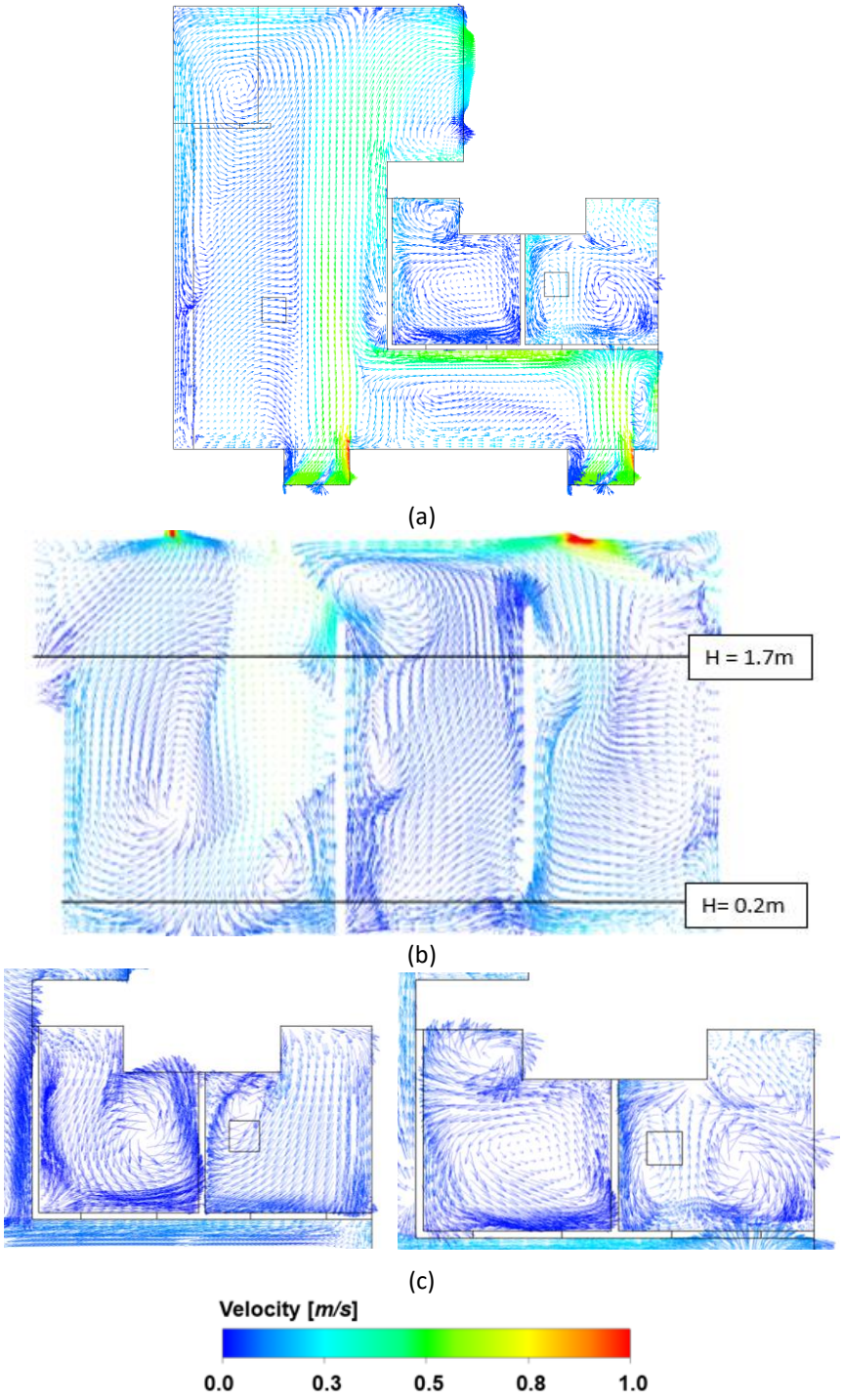

Fig. 9. The distribution of airflow velocity vector in Model 2 (windows are opened) (a) Airflow velocity vectors on the horizontal plane (b) Airflow velocity vectors on the vertical plane (c) Airflow velocity vectors on the horizontal plane at H=1.7m and H=0.2m

In Model 1, the external airflow is notably visible outside the partitions. However, a recirculation area is discernible at the washbasin's location, suggesting that the fresh airflow from the door does not reach this spot. The interior of the partitions displays stable yet weak airflow, with recirculation areas detected both horizontally and vertically. Additionally, airflow direction fluctuates at varying

horizontal heights due to disturbance from external airflow within the partition from above and below.

In Model 2, with windows closed, the airflow within the partitions remains stable and weak, typically registering velocities less than 0.3 m/s. This is attributed to the complex internal structure of Model 2 and the inward positioning of the partitions, which limits their exposure to the external airflow.

Upon opening the window in Model 2, the air inside the model gets influenced by the window's airflow, both within and outside the partitions. Fresh airflow establishes a clear trajectory that propels airflow inside the model, but still doesn't permeate the washbasin area. The interior airflow within the partitions improves considerably compared to when the window is closed, although the overall flow rate inside the partitions remains relatively inconspicuous. The majority of the fresh airflow from the opposing window moves from the top towards the partition containing Monitor Point 1, with a minor portion diverted to the partition housing Monitor Point 2. This creates a significant discrepancy in air residence time between the two partitions, as depicted in Figure 10.

3.4 Distribution of the Residence Time of Air

The simulation results are portrayed through colored contour plots, illustrating the air residence time distributions within the restrooms. These visual representations offer valuable insights into the airflow behavior and help identify areas requiring enhancement.

As depicted in Figure 10, the distribution of air residence time outside the partitions is notably non-uniform across all instances. In Model 1, fresh airflow from outside penetrated deep into the restroom, yet a higher air residence time was observed at the corners, particularly at the washbasin. This is due to the primary alignment of the inflowing air with the door's normal direction, which restricts fresh air from reaching the corners. Conversely, with closed windows in Model 2, the penetration of fresh airflow into the interior was compromised. However, opening the windows improved high residence time areas inside through the introduction of fresh airflow.

Further examination of Figure 10 reveals a longer air residence time within the partitions compared to outside, given that the partitions obstruct overall air exchange and impede the effective influx of fresh air into the cubicle. Despite the existence of a ventilation device, the enhancement of air quality within the partitions remains limited.

Moreover, air quality varies within the two partitions between Model 1 and Model 2 (with windows open), due to differences in the entry method of fresh air into the partitions. In Model 2, with the windows closed, the difference between the two partitions was not substantial, as the airflow from the door was insufficient to enhance air quality in the partition locations.

The figure suggests a likelihood of aerosols lingering in various areas within reference plane 2. The orange and red zones took a minimum of 150 seconds for air refreshment, offering a conducive environment for aerosols to persist, as indicated by the air residence time distribution within the horizontal reference plane. Despite there being only one high-risk region above the left partition in Model 1, prior studies have showcased the COVID-19 virus's propensity to settle in such environments [19-23].

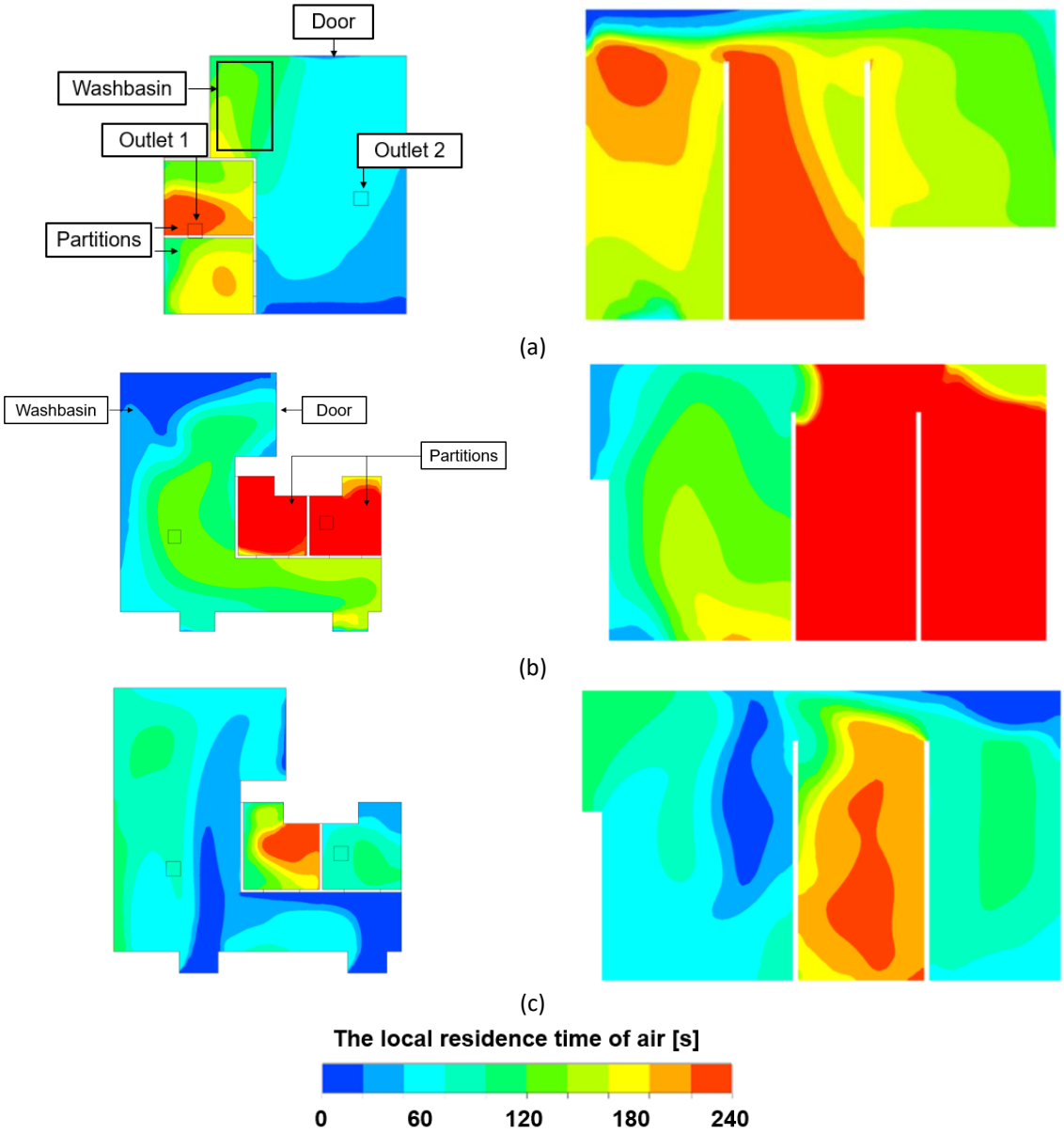

Fig. 10. Distribution of local residence time of air on the reference planes (a) Model 1 (b) Model 2 (windows are closed) (c) Model 2 (windows are opened)

3.5 Variation of Air Residence Time with Time at Two Monitor Points in Each Case

The data presented in Figure 11(a) highlight the prolonged residence time of air within the partitions, especially in areas with complex spatial structures. This extended air residence time raises significant concerns as it could negatively affect the air quality and health of the individuals occupying these spaces. The main cause of this phenomenon is the absence of adequate internal air exchange mechanisms, resulting in static air conditions.

Nonetheless, Figure 11(b) demonstrates that the introduction of additional air exchange inlets can substantially reduce the air's residence time within the partitions. These inlets facilitate the entry of fresh air from the exterior, decreasing indoor air pollutants and enhancing air quality within the partitions. The contrast between the two monitoring points in Figure 10 underlines the significance of adequate air exchange mechanisms, as the airflow direction plays a decisive role in determining the air residence time within the partitions.

In conclusion, the findings illustrated in Figure 11 offer important insights into the significance of air exchange mechanisms for maintaining indoor air quality. They also emphasize the need for proper ventilation systems that are engineered to minimize air residence time within the partitions, thus enhancing the air quality within the compartment's interior.

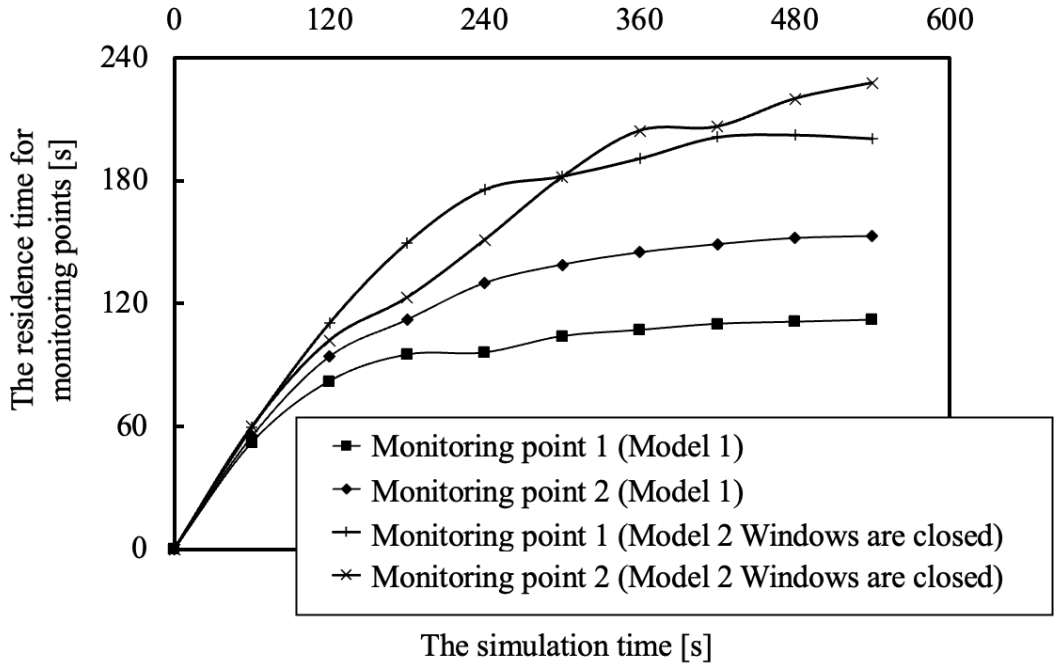

(a)

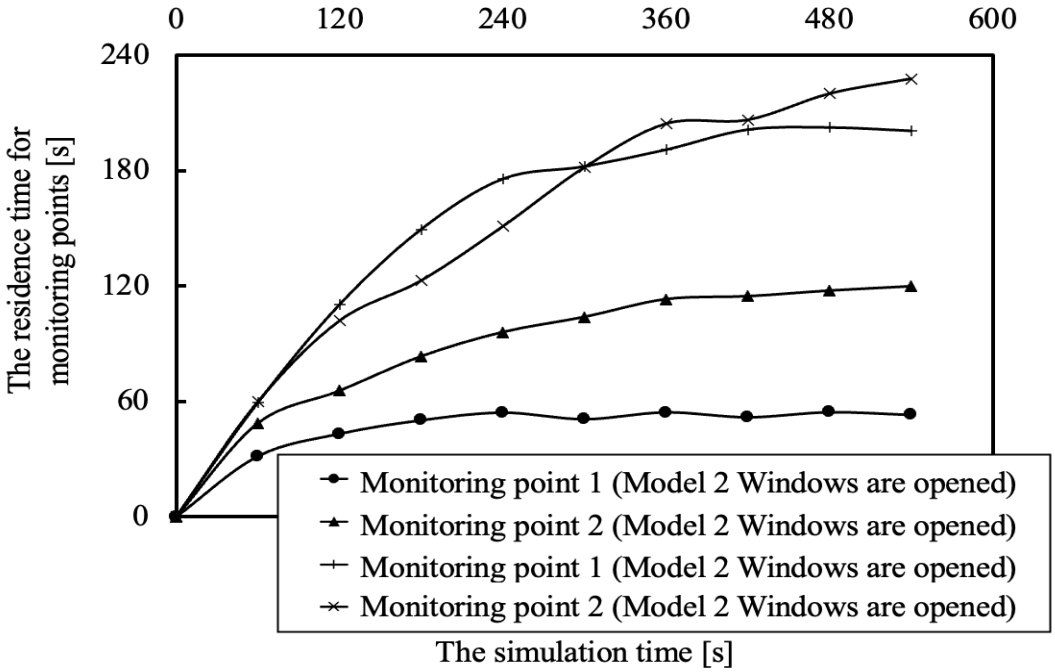

(b)

Fig. 11. The residence time value for two monitor points (a) Comparision between Model 1 and Model 2 (windows closed) (b) Comparision between Model 2 windows closed and opened

4. Conclusions

This study uses air residence time and velocity vector distribution to investigate the ventilation of actual restrooms. A connection between these factors is established by comparing the areas of airflow recirculation with locations of high air residence time. Since aerosol presence indoors is directly tied to these factors, this work illuminates the locations within indoor settings where individuals are most susceptible to COVID-19 infection.

The study's findings present a pragmatic approach to mitigate the risk of airborne virus transmission in restrooms, focusing on specific regions of high air residence time and low air velocity. However, it is crucial to recognize that the results are restricted to the particular restrooms investigated in this study. Therefore, additional research is warranted to assess the influence of ventilation design in various indoor environments.

Moreover, this research supports the idea that enhancing restroom ventilation can aid in preventing the spread of airborne viruses. This becomes especially critical in public facilities such as schools, airports, and hospitals, where large numbers of people gather closely. The findings of this study can guide these facilities to optimize their restroom ventilation systems, thereby reducing the risk of airborne virus transmission.

Beyond ventilation design, other preventive measures such as wearing face masks, frequent hand washing, and maintaining social distancing also play crucial roles in curbing virus transmission. Nonetheless, incorporating effective ventilation design remains paramount in the comprehensive strategy aimed at preventing the spread of airborne viruses in indoor settings.

This research underscores the necessity for further investigations to comprehend the influence of ventilation design on air residence time and the risk of virus transmission across diverse types of indoor environments. Such research can contribute to the formulation of guidelines and best practices for indoor ventilation, thereby safeguarding public health. In essence, this study emphasizes the importance of considering ventilation in controlling airborne virus transmission and advocates for a holistic approach to address this significant public health issue.

Acknowledgement

A part of this research was supported by the Co-Funding Research Program by and between Kyushu Institute of Technology (KYUTECH) and Universiti Putra Malaysia (UPM) 2021-2023.

References

[1] Sinha, Krishnendu, Mani Shankar Yadav, Rajasekharan Jayakrishnan, Guruswamy Kumaraswamy, Janani Srree Murallidharan, and Vivek Kumar. "Field experiments to identify and eliminate recirculation zones to improve indoor ventilation: Comparison with cfd." *Transactions of the Indian National Academy of Engineering* 7, no. 3 (2022): 911-926. https://doi.org/10.1007/s41403-022-00335-1

[2] Bhagat, Rajesh K., MS Davies Wykes, Stuart B. Dalziel, and P. F. Linden. "Effects of ventilation on the indoor spread of COVID-19." *Journal of Fluid Mechanics* 903 (2020): F1. https://doi.org/10.1017/jfm.2020.720

[3] Bolashikov, Zhecho D., Arsen K. Melikov, Wojciech Kierat, Zbigniew Popiołek, and Marek Brand. "Exposure of health care workers and occupants to coughed airborne pathogens in a double-bed hospital patient room with overhead mixing ventilation." *Hvac&R Research* 18, no. 4 (2012): 602-615.

[4] Dbouk, Talib, and Dimitris Drikakis. "On airborne virus transmission in elevators and confined spaces." *Physics of Fluids* 33, no. 1 (2021). https://doi.org/10.1063/5.0038180

[5] Ji, Xiaolin, Olivier Le Bihan, Olivier Ramalho, Corinne Mandin, Barbara D'Anna, Laurent Martinon, Mélanie Nicolas, Denis Bard, and J-C. Pairon. "Characterization of particles emitted by incense burning in an experimental house." *Indoor Air* 20, no. 2 (2010): 147-158. https://doi.org/10.1111/j.1600-0668.2009.00634.x

[6] Wang, Haitao, Miaoda Lin, and Yan Chen. "Performance evaluation of air distribution systems in three different China railway high-speed train cabins using numerical simulation." In *Building simulation*, vol. 7, pp. 629-638. Springer Berlin Heidelberg, 2014. https://doi.org/10.1007/s12273-014-0168-5

[7] Singer, Brett C., Haoran Zhao, Chelsea V. Preble, William W. Delp, Jovan Pantelic, Michael D. Sohn, and Thomas W. Kirchstetter. "Measured influence of overhead HVAC on exposure to airborne contaminants from simulated speaking in a meeting and a classroom." *Indoor air* 32, no. 1 (2022): e12917. https://doi.org/10.1111/ina.12917

[8] Yin, Yonggao, Jitendra K. Gupta, Xiaosong Zhang, Junjie Liu, and Qingyan Chen. "Distributions of respiratory contaminants from a patient with different postures and exhaling modes in a single-bed inpatient room." *Building and environment* 46, no. 1 (2011): 75-81. https://doi.org/10.1016/j.buildenv.2010.07.003

[9] Sinha, Krishnendu, Mani Shankar Yadav, Utkarsh Verma, Janani Srree Murallidharan, and Vivek Kumar. "Effect of recirculation zones on the ventilation of a public washroom." *Physics of Fluids* 33, no. 11 (2021). https://doi.org/10.1063/5.0064337

[10] Zhang, Zhihang, Taehoon Han, Kwang Hee Yoo, Jesse Capecelatro, André L. Boehman, and Kevin Maki. "Disease transmission through expiratory aerosols on an urban bus." *Physics of Fluids* 33, no. 1 (2021). https://doi.org/10.1063/5.0037452

[11] Kassem, Fatma AbdelMordy, Ahmed Farouk AbdelGawad, Ali Elsayed Abuel-Ezz, Mofreh Melad Nassief, and Mohamed Adel. "Design and Performance Evaluation of a Portable Chamber for Prevention of Aerosol Airborne–Infection." *Journal of Advanced Research in Fluid Mechanics and Thermal Sciences* 100, no. 2 (2022): 181-197. https://doi.org/10.37934/arfmts.100.2.181197

[12] Kohanski, Michael A., L. James Lo, and Michael S. Waring. "Review of indoor aerosol generation, transport, and control in the context of COVID-19." In *International forum of allergy & rhinology*, vol. 10, no. 10, pp. 1173-1179. 2020. https://doi.org/10.1002/alr.22661

[13] Noorimotlagh, Zahra, Neemat Jaafarzadeh, Susana Silva Martínez, and Seyyed Abbas Mirzaee. "A systematic review of possible airborne transmission of the COVID-19 virus (SARS-CoV-2) in the indoor air environment." *Environmental research* 193 (2021): 110612. https://doi.org/10.1016/j.envres.2020.110612

[14] Rowe, Bertrand R., André Canosa, Jean-Michel Drouffe, and James Brian Alexander Mitchell. "Simple quantitative assessment of the outdoor versus indoor airborne transmission of viruses and COVID-19." *Environmental research* 198 (2021): 111189. https://doi.org/10.1016/j.envres.2021.111189

[15] Bazant, Martin Z., Ousmane Kodio, Alexander E. Cohen, Kasim Khan, Zongyu Gu, and John WM Bush. "Monitoring carbon dioxide to quantify the risk of indoor airborne transmission of COVID-19." *Flow* 1 (2021): E10. https://doi.org/10.1017/flo.2021.10

[16] Habeebullah, Turki M., Ibrahim HA Abd El-Rahim, and Essam A. Morsy. "Impact of outdoor and indoor meteorological conditions on the COVID-19 transmission in the western region of Saudi Arabia." *Journal of environmental management* 288 (2021): 112392. https://doi.org/10.1016/j.jenvman.2021.112392

[17] Li, Yun-yun, Ji-Xiang Wang, and Xi Chen. "Can a toilet promote virus transmission? From a fluid dynamics perspective." *Physics of Fluids* 32, no. 6 (2020). https://doi.org/10.1063/5.0013318

[18] Toja-Silva, Francisco, Jia Chen, Stephan Hachinger, and Frank Hase. "CFD simulation of CO2 dispersion from urban thermal power plant: Analysis of turbulent Schmidt number and comparison with Gaussian plume model and measurements." *Journal of Wind Engineering and Industrial Aerodynamics* 169 (2017): 177-193. https://doi.org/10.1016/j.jweia.2017.07.015

[19] Rosti, M. E., S. Olivieri, M. Cavaiola, A. Seminara, and A. Mazzino. "Fluid dynamics of COVID-19 airborne infection suggests urgent data for a scientific design of social distancing." *Scientific reports* 10, no. 1 (2020): 22426. https://doi.org/10.1038/s41598-020-80078-7

[20] Yang, Wan, and Linsey C. Marr. "Mechanisms by which ambient humidity may affect viruses in aerosols." *Applied and environmental microbiology* 78, no. 19 (2012): 6781-6788. https://doi.org/10.1038/s41598-020-80078-7

[21] Yang, Wan, and Linsey C. Marr. "Dynamics of airborne influenza A viruses indoors and dependence on humidity." *PloS one* 6, no. 6 (2011): e21481. https://doi.org/10.1371/journal.pone.0021481

[22] Benbough, J. E. "Some factors affecting the survival of airborne viruses." *Journal of General Virology* 10, no. 3 (1971): 209-220. https://doi.org/10.1099/0022-1317-10-3-209

[23] Lednicky, John A., Michael Lauzardo, Md M. Alam, Maha A. Elbadry, Caroline J. Stephenson, Julia C. Gibson, and J. Glenn Morris Jr. "Isolation of SARS-CoV-2 from the air in a car driven by a COVID patient with mild illness." *International Journal of Infectious Diseases* 108 (2021): 212-216. https://doi.org/10.1016/j.ijid.2021.04.063